

Towards a radio-polarimetric study of the bright colliding-wind binary WR 147

A. Blanco¹, P. Benaglia^{1,2}, S. del Palacio² & C. A. Hales³

¹ *Facultad de Ciencias Astronómicas y Geofísicas, UNLP, Argentina*

² *Instituto Argentino de Radioastronomía, CONICET-CICPBA, Argentina*

³ *National Radio Astronomy Observatory, Socorro, USA*

Contact / agustinabelen.blanco@gmail.com

Resumen / Muchos sistemas binarios con colisión de vientos presentan emisión no térmica de radio, la cual se asocia a radiación sincrotrón producida por electrones relativistas. Se espera que esta emisión esté linealmente polarizada, pero dicha polarización aún no ha sido medida. Un estudio polarimétrico en radio nos permitirá inferir la topología del campo magnético en la región de colisión de vientos y así determinar la física de los mecanismos de aceleración que estén actuando en la región. En este trabajo se presentan resultados preliminares de una campaña observacional de sistemas binarios con colisión de vientos, comenzando con WR 147. Como primer paso en el estudio, analizamos la imagen en el parámetro de Stokes I, obteniendo un valor medio para la densidad de flujo de 38.3 ± 1.0 mJy en la banda C y un índice espectral $\alpha = 0.18 \pm 0.05$.

Abstract / Dozens of colliding-wind binaries exhibit non-thermal radio emission which is interpreted as synchrotron radiation produced by relativistic electrons. This emission is expected to be linearly polarized, but such polarization has never been measured. A radio polarimetric study will allow inferring the magnetic field topology in the colliding-winds region, to indirectly assess the physics of the acceleration mechanisms operating there. We conducted a high-sensitivity observational campaign of bright colliding-wind binaries. As a first step in our study, we analysed the Stokes-I parameter in our data set for WR 147. We obtained a flux density of 38.3 ± 1.0 mJy at C-band, and a spectral index $\alpha = 0.18 \pm 0.05$.

Keywords / Polarization — Radiation mechanisms: non-thermal — Radio continuum: stars — Stars: winds, outflows — Stars: individual: WR 147

1. Introduction

Massive, hot stars are commonly found forming stellar systems. In colliding-wind binaries (CWBs), the impact of the powerful stellar winds generates a bright wind collision region (WCR). The subclass of CWBs capable of accelerating particles to relativistic velocities in the WCR is known as particle-accelerating colliding-wind binaries (PACWBs; De Becker & Raucq, 2013).

These sources typically present a composite spectrum in the radio band given by two contributions (De Becker, 2007, and references therein): i) thermal emission from the stellar winds with a canonical spectral index $\alpha \sim 0.6$, and ii) non-thermal synchrotron radiation produced by a population of relativistic electrons spiralling around magnetic field lines, which is also a power law with an intrinsic spectral index $\alpha \sim -0.5$. Typically, thermal emission dominates at high frequencies whereas non-thermal emission dominates at low frequencies. In CWBs, a spectral index $\alpha < 0.6$ is suggestive of a synchrotron contribution to the emission, and negative values of α indicate that this component is dominant. The synchrotron component encodes information on the relativistic electron population and the ambient magnetic field.

Synchrotron radiation is expected to have a high linear polarization (up to $\sim 60 - 70$ %), though no rele-

vant polarization was ever reported from a PACWB. Since polarization is, in principle, directly related to the degree of turbulence in the WCR, its measure would provide important constraints for models on the nature of the radiative and acceleration processes operating in PACWBs.

In a pioneer study, we observed the system WR 146 with the Karl Jansky Very Large Array (JVLA) and obtained an upper limit of 0.6 % fractional polarization across 1–8 GHz (Hales et al., 2017). This could suggest i) a highly disordered magnetic field –thus favouring a scenario in which particles are accelerated by turbulent magnetic reconnection instead of diffusive shock acceleration; ii) that relevant depolarization effects are at work (e.g. Sokoloff et al., 1998, and references therein); iii) a combination of both.

We intend to extend our study to five of the most powerful PACWBs, selected from the catalogue by De Becker & Raucq (2013), which are listed in Table 1. For this purpose, we obtained high-sensitivity (expected rms $< 100 \mu\text{Jy}$) polarimetric observations at L and C bands with the JVLA. As a first step in the analysis, we present here preliminary C-band Stokes-I results for the system WR 147.

Table 1: Observed targets in project 16A-252. The flux density and spectral index values are taken from De Becker & Raucq (2013). Quoted values are for reference only, as orbital variability is expected.

System name	$S_{5\text{cm}}$ [mJy]	$\alpha_{5\text{cm}}$
WR 147	35.4 ± 0.4	0.05
WR 140	≤ 28.1	-0.27
HD 167971	17.1 ± 0.4	-0.48
HD 168112	5.64 ± 0.13	-0.78
9 Sgr	2.8 ± 0.4	-1.1

2. WR 147

The massive system WR 147 is located at a distance of 0.65 kpc, in the Cygnus OB2 region. Its components, of spectral types WN8(h)+B0.5V, are separated by $0.64''$. It was mapped in radio, IR and optical wavelengths (Skinner et al., 1999, and references therein), and resolved in X-rays (Pittard et al., 2002).

MERLIN observations at 5 GHz (Williams et al., 1997) show thermal emission from a southern source, associated with the stellar wind from the WN8 star, and a non-thermal northern source located in the region where the WN8 stellar wind collides with the weaker wind of the OB star.

Table 2: Parameters of the WR 147 system for the primary (sub-index 1) and the secondary (sub-index 2) components (see Setia Gunawan et al., 2001, and references therein).

Parameter	Value	Unit
Primary spectral type	WN8(h)	
Wind terminal velocity $v_{\infty 1}$	950	km s^{-1}
Mass-loss rate \dot{M}_1	2.4×10^{-5}	$M_{\odot} \text{ yr}^{-1}$
Secondary spectral type	B0.5 V	
Wind terminal velocity $v_{\infty 2}$	800	km s^{-1}
Mass-loss rate \dot{M}_2	4×10^{-7}	$M_{\odot} \text{ yr}^{-1}$
Distance	0.65	kpc
System separation	643 ± 157	mas
Period	1350	yr
Wind momentum ratio	$\eta = 0.014$	

3. Observations and data reduction

We performed radio continuum observations of five PACWBs using the JVL A in August 2016, under Project Code 16A-252. Full polarization observations were carried out in B-configuration array at two frequency bands centred at 1.5 GHz (20 cm, L band) and 6 GHz (5 cm, C band), spanning bandwidths of 1 GHz and 4 GHz, respectively. In the 20 cm band, the correlator was configured to deliver 8 spectral windows with 64×1 MHz channels. The 5 cm band was configured to deliver 32 spectral windows with 64×2 MHz channels. The time sampling was 3 s for both bands. The total (on source) observing time on WR 147 was 45 min at L band and 15 min at C band. We observed 3C 286 for the purpose of absolute flux density and position angle calibrations, J2007+404 for complex gain calibration, and J2355+4950 for leakage calibration.

The C-band data were reduced using version 5.3.0 of the CASA package. Hanning smoothing was performed. RFI and bad data were identified manually and conservatively flagged. We imaged the total intensity for the 5 cm band, as well as per sub-band, binning every 8 spectral windows out of 32 (i.e., four subsets of 1 GHz width each); the three windows that were most affected by RFI belong to the third data subset.

4. Preliminary results

The source was detected with a signal-to-noise ratio of ~ 300 , a peak flux of $26.38 \text{ mJy beam}^{-1}$ and a rms noise of $0.09 \text{ mJy beam}^{-1}$. A gaussian fit provided an integrated flux value of $38.3 \pm 1.0 \text{ mJy}$.

The radio peak is in excellent agreement with the optical position given for instance by Morris et al. (2000). Since the angular resolution of the present observations is $\sim 1''$, we cannot discriminate the different components that contribute to the detected emission (i.e., the individual stellar winds and the WCR).

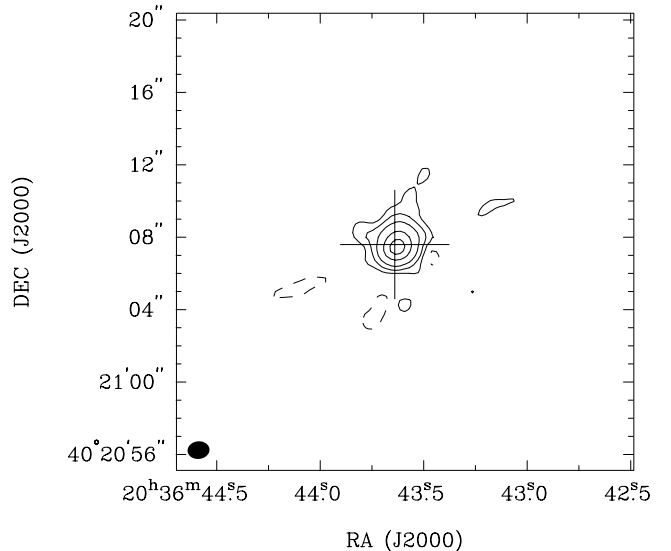


Figure 1: Continuum (Stokes I) robust-weighted ($\text{robust}=0.5$) image of WR 147 with the JVL A at C-band. The position of WR 147 is marked with a cross. The synthesized beam-width size is $1.21'' \times 0.97''$ with $PA = -83.8^\circ$ (shown at the bottom left corner). The pixel size is $0.25''$ and the image size is 2400×2400 pixels. Contour levels are -0.3, 0.3, 1, 3, 10, and 20 mJy beam^{-1} .

In addition, the large bandwidth at C band allows us to inspect flux variations in frequency and to do a preliminary analysis of the spectral index. With this purpose, we computed the total flux in four sub-bands of width ~ 1 GHz centered at 4.5, 5.5, 6.5, and 7.5 GHz. The best fit of a power-law to this data set yields $\alpha = 0.18 \pm 0.05$ (Fig. 2). This spectral index is consistent with a composed spectrum of thermal emission from the stellar winds (with canonical value $\alpha \sim 0.6$) and non-thermal emission from the WCR (with canonical value $\alpha \sim -0.5$).

As a consistency check, we estimate the expected flux from the ionized stellar winds; such an estimate is reliable only within a factor 2–3 due to uncertainties in the wind parameters. In this system, the thermal emission is expected to be completely dominated by the primary star, as it has a much larger mass-loss rate. Assuming an rms ionic charge of $\gamma = 1$, a mean atomic weight of $\mu \approx 2$, and a volume filling factor of $f = 0.1$, the estimated thermal flux density at 4 GHz is ≈ 6 mJy and at 8 GHz is ≈ 10 mJy (see e.g. De Becker, 2018, and references therein). This estimate is consistent with the interpretation of a composite thermal plus non-thermal spectrum.

We aim to achieve a precise decomposition of the spectrum in its components when the L-band data is added to the analysis. The determination of the spectral index of the non-thermal component at low frequencies, α_{NT} , will allow us to characterize the relativistic electron distribution, which is a power law with spectral index $p = -2\alpha_{\text{NT}} + 1$. The subsequent modelling of the synchrotron spectrum will allow us to provide constraints on the magnetic field intensity and the acceleration efficiency in the WCR (e.g. del Palacio et al., 2016; Hales et al., 2017; De Becker, 2018).

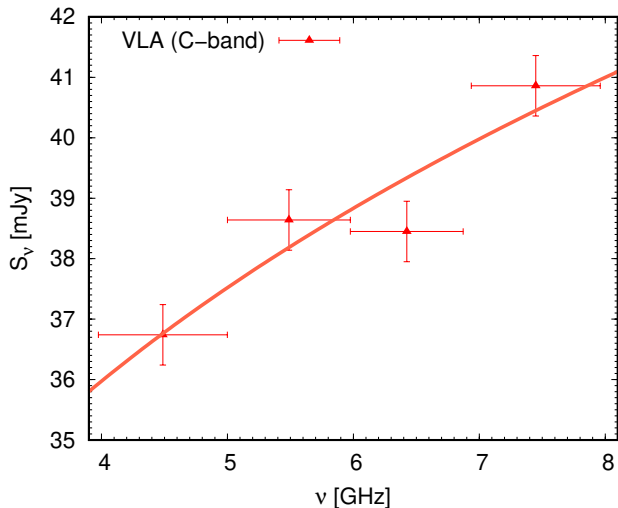


Figure 2: Spectral energy distribution of WR 147 taking four sub-bands within C-band.

5. Conclusions

We presented preliminary results on the analysis of radio polarimetric observations of the system WR 147 as part of an ongoing investigation of the polarized synchrotron emission from PACWBs. As a first product of these observations, we obtained an intensity map and spectral energy distribution for the source. The large bandwidth available with the JVLA allowed for a first estimate of the spectral index within the C band, though a more reliable determination will be possible with the addition of the L-band data in the future. The high signal-to-noise ratio of the observations suggests that we should be able to detect even a small fraction ($\lesssim 3\%$) of linear

polarization, if present. Moreover, the large frequency range covered by our observations will allow us to look for frequency-dependent depolarization. We thus expect to set very tight constraints to the polarization in the radio emission from WR 147, giving further insight on the magnetic field topology in the WCR from luminous PACWBs.

Acknowledgements: A.B and P.B. acknowledge support from AN-PCyT PICT 2017-0773, Facultad de Ciencias Astronómicas y Geofísicas (UNLP) and Asociación Argentina de Astronomía. The National Radio Astronomy Observatory is a facility of the National Science Foundation operated under cooperative agreement by Associated Universities, Inc.

References

- De Becker M., 2007, *A&A Rv*, 14, 171
- De Becker M., 2018, *A&A*, 620, A144
- De Becker M., Raucq F., 2013, *A&A*, 558, A28
- del Palacio S., et al., 2016, *A&A*, 591, A139
- Hales C.A., et al., 2017, *A&A*, 598, A42
- Morris P.W., et al., 2000, *A&A*, 353, 624
- Pittard J.M., et al., 2002, *A&A*, 388, 335
- Setia Gunawan D.Y.A., et al., 2001, *A&A*, 368, 484
- Skinner S.L., et al., 1999, *ApJ*, 524, 394
- Sokoloff D.D., et al., 1998, *MNRAS*, 299, 189
- Williams P.M., et al., 1997, *MNRAS*, 289, 10